

# Microbial methane formation in deep aquifers associated with the sediment burial history at a coastal site

Taiki Katayama<sup>1</sup>, Reo Ikawa<sup>2</sup>, Masaru Koshigai<sup>2</sup>, Susumu Sakata<sup>1</sup>

<sup>1</sup>Geomicrobiology Research Group, Institute for Geo-Resources and Environment, Geological Survey of Japan (GSI), National Institute of Advanced Industrial Science and Technology (AIST), 1-1-1 Higashi, Tsukuba, 305-8567, Japan.

<sup>2</sup>Groundwater Research Group, Institute for Geo-Resources and Environment, GSI, AIST, 1-1-1 Higashi, Tsukuba, 305-8567, Japan.

Correspondence to: Taiki Katayama (katayama.t@aist.go.jp) and Susumu Sakata (su-sakata@aist.go.jp)

**Abstract.** Elucidating the mechanisms underlying microbial methane formation in subsurface environments is essential to understanding the global carbon cycle. This study examined how microbial methane formation (i.e., methanogenesis) occurs in natural gas-bearing sedimentary aquifers throughout the sediment burial history. Water samples collected from six aquifers of different depths exhibited ascending vertical gradients in salinity from brine to freshwater and in temperature from mesophilic to psychrophilic conditions. Analyses of gas and water isotopic ratios and microbial communities indicated the predominance of methanogenesis via CO<sub>2</sub> reduction. However, the hydrogen isotopic ratio of water changed along the depth and salinity gradient, whereas the ratio of methane changed little, suggesting that in situ methanogenesis in shallow sediments does not significantly contribute to methane in the aquifers. The population of methane-producing microorganisms (methanogens) was highest in the deepest saline aquifers, where the water temperature, salinity, and total organic carbon content of the adjacent mud sediments were the highest. Cultivation of the dominant hydrogenotrophic methanogens in the aquifers showed that the methanogenesis rate was maximized at the temperature corresponding to that of the deepest aquifer. These results suggest that high-temperature conditions in deeply buried sediments are associated with enhanced in situ methanogenesis and that methane that forms in the deepest aquifer migrates upward into the shallower aquifers by diffusion.

## 1 Introduction

Terrestrial subsurface environments are massive reservoirs of water and organic matter, where microbial processes drive geochemical cycling (Lovely and Chapelle, 1995; McMahon and Parnell, 2014). Aquifers that form in sedimentary environments provide microorganisms with pore spaces, water, and buried organic materials that serve as energy and carbon sources, thereby sustaining metabolic activity and influencing the organic and inorganic geochemistry of subsurface environments (McMahon and Chapelle, 1991; Lovley and Chapelle, 1995; Fredrickson et al., 1997; Krumholz et al., 1997).

Methanogenesis, the process of methane formation by methanogens, represents a terminal step in the degradation of organic matter in anoxic environments (Lovely and Chapelle, 1995). Methanogens form a diverse group of archaea that produce methane from various substrates, including H<sub>2</sub> and CO<sub>2</sub> (hydrogenotrophic), methylated compounds (methylotrophic), acetate (acetoclastic), methoxylated aromatic compounds (Mayumi et al., 2016) or alkanes (Zhou et al., 2022). Because active methanogens are widespread in subsurface environments (Mesle et al., 2013), it has been speculated that microbial methane

スタイル定義: EndNote Bibliography Title: フォント: 10 pt

スタイル定義: EndNote Bibliography: フォント: 10 pt

スタイル定義: コメント文字列: フォント: (英) Tahoma, 8 pt

削除:

削除:

削除: understand

削除: and to explore natural gas deposits.

削除: .

書式を変更: 英語 (米国)

書式を変更: 英語 (米国)

書式を変更: フォント: 斜体 (なし)

削除: the

削除: the

削除: that dominated

削除: ,

削除: formed

削除: upwards

削除:

削除: ,

削除: they harbor a large fraction of the microorganisms present on Earth (...)

削除: ; Magnabosco et al., 2018).

削除: formed

削除: the

削除: biological

削除: , is

削除: process involving

削除: where electron acceptors other than CO<sub>2</sub> are depleted.

削除: comprise

削除: or

may comprise a larger proportion of natural gas reserves than previously thought (Kotelnikova, 2002). In addition to methanogenesis, recent research has shed light on the process of methane formation by certain nonmethanogenic microbes, including cyanobacteria, algae, fungi, purple nonsulfur bacteria, and cryptogamic covers, which occur in oxygen-saturated aquatic and terrestrial ecosystems (Liu et al., 2022).

The sedimentary aquifers explored in this study are located beneath the Teshio Plain, in a coastal area of northern Japan (Fig. S1). Isotopic analysis of hydrocarbon gases in this area has revealed that methane predominates over ethane and propane, thus suggesting a microbial origin for natural gases (Tamamura et al., 2014). Ikawa et al. (2014), who conducted geochemical analyses of porewaters extracted from sediment core samples from the D-1 borehole, drilled to a depth of 1,000 m below the ground surface (mbgs) of the plain, and they found vertical gradients of the Cl<sup>-</sup> concentration and the hydrogen isotopic ratio of water (Fig. 1b, c). They proposed the following processes to explain how these gradients formed. Sediments corresponding to the Yuchi Formation were deposited in shallow, marine environments during the late Pliocene Epoch. Deposition of the sediments corresponding to the Sarabetsu Formation, which overlies the Yuchi Formation, occurred in bay, lagoon, or fluvial environments during the early Pleistocene Epoch. Brackish and fresh waters trapped during this period became mixed with brine from the Yuchi Formation by diffusion, resulting in the formation of a continuous vertical salinity gradient. Aquifers within the upper part of the Sarabetsu Formation (90–280 mbgs) were recharged with paleo-meteoric water. Throughout the burial history of the Yuchi Formation, temperature increased along the geothermal gradient (Fig. 1d). Therefore, aquifers in the Yuchi Formation provide an opportunity to explore the impacts of these geochemical changes on microbial methane formation.

削除: Microbial methane has been estimated to account for more than 20% of global natural gas resources (Katz, 2011)

削除: ,

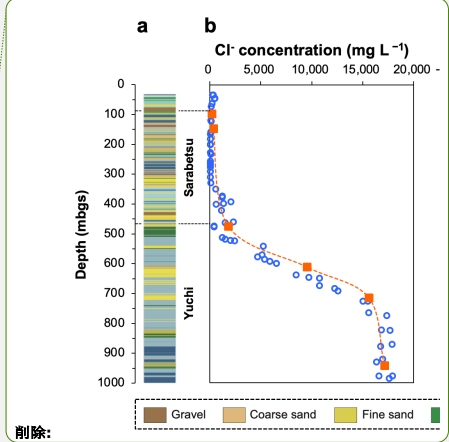
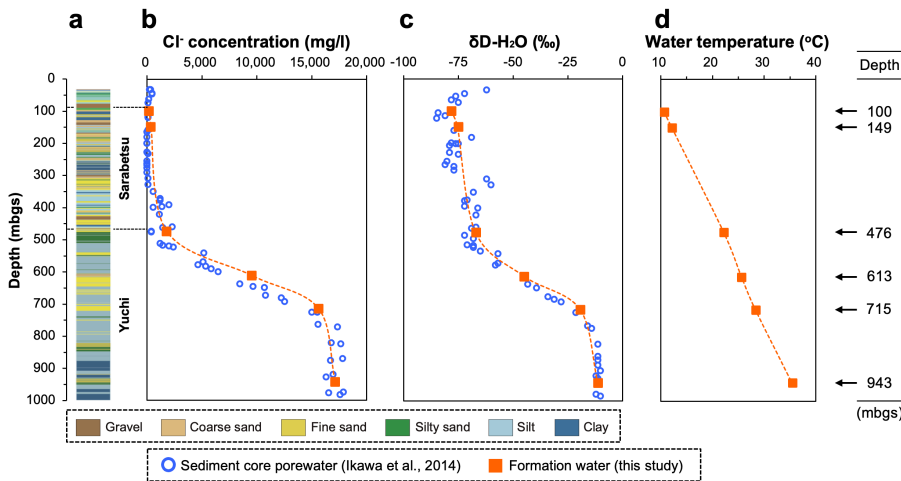
削除: the

削除: -

削除: ,

削除: water salinity decreased while

削除:



削除:

**Figure 1.** Depth profiles of borehole D-1: (a) lithology, (b)  $\text{Cl}^-$  concentration, (c) hydrogen isotopic ratio, and (d) temperature of sediment core porewater (blue open circles) (data from Ikawa et al., 2014) and water samples from the aquifers investigated in this study (orange solid squares). The aquifer depths at which the waters were sampled are shown on the right.

In this study, water samples were collected from the saline aquifers in the Yuchi Formation at 476 (fine sand), 613 (coarse sand), 715 (fine sand), and 943 (fine sand) mbgs, and from the freshwater aquifers in the upper part of the Sarabetsu Formation at 100 (coarse sand) and 149 (coarse sand) mbgs, as reference material for the Yuchi Formation samples (Fig. 1). Whereas many previous studies have conducted geologic and geochemical analyses to examine the relationship between the burial history of geological formations and the occurrence of methane deposits [e.g., Zhang et al., 2013, and references therein], this study combines microbiological analyses (e.g., gene sequencing and cultivation-based analyses) with geochemical analyses to elucidate this relationship from multiple perspectives.

## 2 Materials and methods

### 2.1 Site description and sample collection

The study site was located on a sand dune 300 m from the coastline of the Teshio Plain located in northern Hokkaido (44.9948° N, 141.6882° E) at an elevation of 5.2 m above sea level (Fig. S1). The geology of this site down to a depth of 1,000 mbgs consists of the Yuchi Formation, the Sarabetsu Formation, and alluvium, in ascending order. Hydraulic gradient and conductivity, water isotopic, and geological data indicate that clay aquitards at approximately 300 mbgs prevent water in the upper part of the Sarabetsu Formation from mixing with connate water in the lower part of the Sarabetsu Formation and the underlying Yuchi Formation (Ikawa et al., 2014). Indeed, a drastic change observed in the stable hydrogen ( $\delta\text{D}$ ) isotope ratio of the water at approximately 300 mbgs (Fig. 1c) indicates that the aquifers above and below that depth are hydrologically different (Ikawa et al., 2014).

The water samples for this study were collected from three wells: D-1, D-2, and D-3. The D-2 and D-3 wells are located within 30 m of D-1. Two samples from D-2 and D-3 are freshwater derived from the upper Sarabetsu Formation, and four samples from D-1 are brines derived from the Yuchi Formation. Samples from D-2 and D-3 were pumped through strainers at depths of 90-100 mbgs and 130-149 mbgs, respectively, while samples from D-1 were pumped with borehole packer assemblies at depths of 476, 613, 715 and 943 mbgs. The water samples were obtained after chemical parameters, such as the water temperature, electrical conductivity, pH, and oxidation-reduction potential, had stabilized. Before sample collection, waters of approximately 44-160 times the wellbore volume of D-2 or D-3 and 4-13 times the packer-sealed area of D-1 were pumped out.

Water samples for microbial cultures were collected in sterilized glass bottles with butyl rubber stoppers and screw caps. The bottles were purged with  $\text{N}_2$  gas before and during sample collection and then filled with the water sample to raise the internal pressure of the bottles, effectively preventing the penetration of air. For the molecular analysis, 4-L water samples were collected and filtered through a 0.2- $\mu\text{m}$ -pore-size Millipore Express Plus membrane filter (Millipore, Billerica, MA, USA) and stored at  $-20^\circ\text{C}$ . The samples used for total cell counts were fixed with formalin at a final concentration of 2%

削除: at

削除: (

削除: ,

削除: ,

削除: ,

削除: )

書式を変更: フォントの色: 黒

削除: (

削除: ),

削除: .

削除: . (

削除: )

削除: .

削除: -

削除: 44.9948° N, 141.6882° E) (

削除: the

削除: ,

削除: freshwaters

削除: the

削除: the

削除: -

削除: the

削除: the

削除:

削除: Samples

削除: the

削除: maintain

削除: samples under anaerobic conditions

(v/v) immediately after sampling and stored at 4 °C. The gases that were associated with the formation water in aquifers (i.e., under high-pressure conditions) were naturally separated from the water when it was sampled under atmospheric pressure. These separated gases were collected using the water displacement method.

削除: and

削除: at the time of sampling

削除: over

150

## 2.2 Geochemical analysis

The chemical compositions and stable hydrogen isotope ratios ( $\delta D$ ) of the water samples were measured by using ion chromatography (DIONEX ICS-5000, Thermo Fisher Scientific, Bremen, Germany) and a liquid water isotope analyzer (L2120-i, Picarro, Santa Clara, CA, USA), respectively. The standard deviation of  $\delta D$  for water was 1‰.

155

The gas composition was analyzed using two gas chromatographs: a Shimadzu GC-8A equipped with a thermal conductivity detector and a Molecular Sieve 5A column and an Agilent 6890 equipped with a flame ionization detector and a PoraPLOT Q column. Stable carbon ( $\delta^{13}C$ ) and hydrogen ( $\delta D$ ) isotope ratios of methane, along with the  $\delta^{13}C$  of carbon dioxide, were measured using a Trace Ultra gas chromatograph connected to a DELTA V plus isotope ratio mass spectrometer (IRMS) through a GC IsoLink combustion/pyrolysis interface (Thermo Fisher Scientific), and the column was a PoraPLOT Q. The Natural Gas Standard NGS3 was used as an isotope reference material. The standard deviations of  $\delta D$  and  $\delta^{13}C$  for methane were 1.6‰ and 0.3‰, respectively, and the standard deviation of  $\delta^{13}C$  for carbon dioxide was 0.2‰.

削除: measured by

削除: a

削除: chromatograph (

削除: )

削除: -

削除: thermal conductivity detector (TCD). The stable

削除: and

削除: with

削除: via

削除: )

削除: )

削除: 1M

削除:

165

## 2.3 Direct cell counts

A fixed water sample was filtered through a 0.2- $\mu m$ -pore-size Isopore membrane filter (Millipore), stained for 10 min with SYBR Green solution (10  $\mu g mL^{-1}$ ), and observed under an epifluorescence microscope (Olympus, Tokyo, Japan).

削除:

170

## 2.4 DNA extraction and quantitative PCR for 16S rRNA and *mcrA* genes

DNA was extracted from the filtered water and methanogenic culture (as described below) samples by using a PowerWater kit (MoBio Laboratories, CA, USA) according to the manufacturer's protocol. Quantitative PCR targeting bacterial and archaeal 16S rRNA genes in water samples was performed in triplicate by the quenching probe method (Tani et al., 2009) using TITANIUM Taq DNA polymerase (Takara, Otsu, Japan) in a Rotor-Gene Q real-time cyclor (QIAGEN, Valencia, CA).

175

The primers and probes used for real-time PCR and sequencing (as described below) are listed in Table S1. The cycling conditions were 95 °C for 2 min, followed by 50 cycles of 93 °C for 15 s, 61 °C for 20 s, and 72 °C for 25 s. The copy numbers of the *mcrA* gene, which encodes a methyl-coenzyme M reductase alpha subunit, an enzyme central to methanogenesis, were quantified in triplicate by SYBR Green real-time PCR using SYBR Premix Ex-Taq II (Takara) in a LightCycler 1.0 (Roche, Basel, Switzerland). The cycling conditions were 95 °C for 30 s, followed by 50 cycles of 95 °C for 15 s, 52 °C for 20 s, and 72 °C for 25 s. Tenfold serial dilutions of the target PCR products for *Escherichia coli* K12 (ATCC 10798) (for the bacterial

削除: a

削除: the

削除: a

削除: Ten-fold

180

16S rRNA gene) and *Methanobacterium bryantii* M.o.H. (ATCC 33272) (for the archaeal 16S rRNA and *mcrA* genes) were also amplified to calculate the gene copy numbers.

## 205 2.5 454 pyrosequencing of 16S rRNA genes

The 16S rRNA genes, including the V3 and V4 regions, were amplified using AmpliTaq Gold 360 DNA polymerase (Life Technologies, CA, USA) with a Univ515F primer (fused to the 454-specific adaptor A and 6-nt barcode sequences) and a Univ926R primer (fused to adaptor B). The cycling conditions were 95 °C for 10 min, followed by 25–27 cycles of 95 °C for 30 s, 50 °C for 40 s, and 72 °C for 30 s, and a final extension period of 7 min at 72 °C. Four replicates of PCR products for each sample were pooled and purified by using a MonoFas DNA purification kit. Pyrosequencing was performed using a 454 Life Sciences GS FLX Titanium platform (Roche, Basel, Switzerland) at Hokkaido System Science Co., Ltd. (Sapporo, Japan).

削除:

削除: Cycling

書式を変更: フォントの色: 黒

削除: the

## 2.6 Cloning and Sanger sequencing of the *mcrA* gene

The *mcrA* gene was amplified from the six original water and methanogenic culture samples (as described below) by using the MLf and MLr primer pair (Luton et al., 2002) and AmpliTaq Gold 360 DNA Polymerase (Thermo Fisher Scientific). The PCR products were purified by using a MonoFas DNA purification kit (GL Sciences, Tokyo, Japan), cloned in the pCR4-TOPO vector (Thermo Fisher Scientific), and sequenced by the dideoxynucleotide chain-termination method using BigDye terminator reagents (Thermo Fisher Scientific) and an automated sequence analyzer (3730 DNA Analyzer, Thermo Fisher Scientific) according to the manufacturer's instructions.

削除: ThermoFisher

削除: ThermoFisher

削除: ThermoFisher

削除: ThermoFisher

削除:

## 2.7 Sequence analysis

The 454 pyrosequencing reads of the 16S rRNA genes were analyzed by using Mothur ver. 1.48 software (Schloss et al., 2009), as described previously (Katayama et al., 2015, 2022) with the following modifications. Quality-filtered sequences with an average length of 250 bp were classified by using a Bayesian classifier based on the Silva taxonomy SSU Ref 138.1 dataset (Pruesse et al., 2007) with a confidence threshold of 80%. The putative methanogens in the 16S rRNA gene sequences were searched based on this taxonomic classification.

削除: )

削除:

削除: acid in silico

Sanger sequences of the *mcrA* gene were translated to amino acids and aligned by using MAFFT ver. 7 software (Katoh and Standley, 2013). Amino acid sequences with >93% sequence identity were treated as operational taxonomic units (OTUs).

In each OTU, the most abundant sequence was selected as the representative sequence. The species most closely related to the OTUs were searched by using BLAST (<http://blast.ncbi.nlm.nih.gov/Blast.cgi>).

削除: species

The 454-sequencing data were submitted to the DDBJ Sequence Read Archive database under accession number DRA001113. The GenBank/EMBL/DDBJ accession numbers for the *mcrA* gene sequences are LC214911 to LC214935.

## 2.8 Cultivation of methanogens

The basal medium used for the methanogenic cultures consisted of 10 mM NH<sub>4</sub>Cl, 1 mM KH<sub>2</sub>PO<sub>4</sub>, 15 mM MgCl<sub>2</sub>·6H<sub>2</sub>O, 1 mM CaCl<sub>2</sub>·2H<sub>2</sub>O, 30 mM NaHCO<sub>3</sub>, 1 mL L<sup>-1</sup> selenium and tungsten solution, 1 mL L<sup>-1</sup> trace element solution, 2 mL L<sup>-1</sup> vitamin solution, 1 mL L<sup>-1</sup> resazurin solution (1 mg mL<sup>-1</sup>), and 0.5 mM titanium(III) nitrioltriacetate (as a reducing agent) (Katayama and Kamagata, 2018; Katayama et al., 2020). Twenty milliliters of basal mineral medium was dispensed into 67-mL serum vials. The vials were sealed with butyl rubber septa and aluminum crimps under an atmosphere of N<sub>2</sub>/CO<sub>2</sub> (80:20, v/v). The medium was supplemented with either H<sub>2</sub>/CO<sub>2</sub> (80:20, v/v; 0.1 MPa) or acetate (20 mM) as methanogenic substrates. The medium was further supplemented with NaCl at final concentrations of 250 and 500 mM, which approximated its in situ concentrations at 613 and 943 mbgs, respectively. One-milliliter aliquots of the water samples from 613 and 943 mbgs were dispensed into each medium and incubated at 25 °C (for the 613-mbgs sample) and 35 °C (for the 943-mbgs sample) to approximate the in situ water temperature. Methane production was measured using a GC equipped with a TCD. After methane production was terminated, 4 mL of the sample cultures were harvested by filtration, and the *mcrA* gene was cloned and sequenced as described above.

删除: of

删除: of

删除: elements

删除: of

删除: of

250

255

260

### 2.9 Effects of salinity and temperature on methanogenesis

Methane-producing cultures supplemented with H<sub>2</sub>/CO<sub>2</sub> or acetate from the 943-mbgs water sample were subsequently inoculated into fresh media to examine the methanogenic activity under different salinity and temperature conditions. Cultures with different salinities were grown in basal mineral media containing 15, 270, or 480 mM Cl<sup>-</sup> at 35 °C. Cultures with different temperatures were grown in basal mineral media containing 480 mM Cl<sup>-</sup> at 20, 25, 35, or 45 °C. Both culture sets were supplemented with H<sub>2</sub>/CO<sub>2</sub> (80:20, v/v; 0.1 MPa) or acetate (20 mM). The time course for methane production was determined to calculate the methane production rate.

删除: medium

删除: a

删除: medium

删除: medium

265

删除:

### 2.10 Cultivation of microorganisms syntrophically oxidizing acetate to methane

Semicontinuous cultivation supplemented with a low concentration of acetate (0.4 mM) was performed in a modified 132-mL glass vial containing sterilized pieces of nonwoven fabric as the carrier material for microbial cells (Fig. S2a) to culture microorganisms involved in syntrophic acetate oxidation (SAO) coupled to methanogenesis via carbonate reduction. Forty milliliters of basal mineral medium (as described above) supplemented with NaCl (500 mM) and acetate (0.4 mM) was dispensed into the vial. Ten milliliters of the 943-mbgs water sample was used as an inoculum. The top and bottom of the vial were sealed with a butyl rubber septum and aluminum crimps, and the culture was incubated at 35 °C under an N<sub>2</sub>/CO<sub>2</sub> (80:20, v/v) atmosphere for 10 months. During cultivation, the culture was manually fed acetate (0.4 mM) at 3-week intervals. Before feeding, 20 mL of culture liquid was removed from the vial through the bottom septum using a needle syringe, and 20 mL of fresh medium containing acetate (final concentration: 0.4 mM) was then added to the vial through the top septum so that the syntrophic association of microbial cells was not physically disrupted by turning the vial upside down.

删除: microorganisms

删除: Semi-continuous

删除: non-woven

270

275

删除: with

删除:

删除: non-woven

删除: semi-continuous

删除: non-labeled

280

After cultivation, 2 mL of culture liquid and a piece of nonwoven fabric were transferred from the semicontinuous cultivation system to 67-mL serum vials containing basal mineral medium with 0.4 mM [2-<sup>13</sup>C]-acetate or nonlabeled acetate

300 (used as a control) to determine the presence of SAO activity. In both cultures, 0.4 mM labeled or unlabeled acetate supplement was added at 2-week intervals. The incubation was performed in duplicate. Time courses for methane production and the stable carbon isotopic ratio of dissolved inorganic carbon (DIC) in the culture liquid were determined by using GC and GC/IRMS, respectively, as described above.

删除: a

删除: a

### 305 3 Results

#### 3.1 Geochemistry of water and sediment

The geochemical properties of the six water samples are summarized in Tables 1 and 2. The redox potentials in the freshwater samples from the upper Sarabetsu Formation aquifers (100 and 149 mbgs) were higher ( $> -210$  mV) than those in the brine samples from the Yuchi Formation aquifers (476, 613, 715, and 943 mbgs) ( $< -290$  mV).  $\text{NO}_3^-$  and  $\text{SO}_4^{2-}$  were detected only in the upper Sarabetsu Formation samples, but mostly in small amounts not exceeding  $1.4 \text{ mg L}^{-1}$ . The water temperature increased with depth ( $r > 0.99$ ,  $p < 0.001$ ; linear regression  $t$ -test) and ranged from  $10.6$  to  $35.4$  °C. Stiff diagrams showed a difference in water chemistry between the upper Sarabetsu and Yuchi Formation samples (Fig. S3), which is consistent with hydrologic separation above and below the clay aquitards (Ikawa et al., 2014). The  $\text{Cl}^-$  concentrations and  $\delta\text{D-H}_2\text{O}$  values of all six water samples were similar to those of porewater within the sediment cores at the corresponding depths (Fig. 1); thus, they showed no sign of cross-contamination among the samples.

删除: ,

删除: -

删除: show

删除: the

315 In all water samples,  $\text{CH}_4$  accounted for  $>75\%$  of the total dissolved gas (Table 2). The proportions of  $\text{CH}_4$  and  $\text{CO}_2$  increased with depth, whereas that of  $\text{N}_2$  decreased. The stable carbon ( $\delta^{13}\text{C}$ ) and hydrogen ( $\delta\text{D}$ ) isotopic ratios of methane ranged from  $-77.1\%$  to  $-67.5\%$  and from  $-258\%$  to  $-196\%$ , respectively. Among the samples from the Yuchi Formation, changes in  $\delta\text{D-CH}_4$  values were small ( $7\%$ ) compared with changes in  $\delta\text{D-H}_2\text{O}$  values ( $56\%$ ) (also evident in Fig. 2c). Plots of the isotopic ratios of the gases and water, i.e.,  $\delta^{13}\text{C-CH}_4$  versus  $\delta\text{D-CH}_4$ ,  $\delta^{13}\text{C-CO}_2$  versus  $\delta^{13}\text{C-CH}_4$ , and  $\delta\text{D-CH}_4$  versus  $\delta\text{D-H}_2\text{O}$  (Whiticar, 1999) (Fig. 2a–c), indicated a microbial origin of dissolved methane via the  $\text{CO}_2$  reduction pathway in both the upper Sarabetsu and the Yuchi Formation samples. Methane dissolved in water from the Koetoi Formation, which underlies the Yuchi Formation (Fig. S1), plotted near the boundary between a biogenic and a thermogenic origin (Tamamura et al., 2014) (Fig. 2a). The isotopic difference indicates that the proportion of methane in the upper Sarabetsu and Yuchi Formations derived from the lower Koetoi Formation was minimal.

删除: show

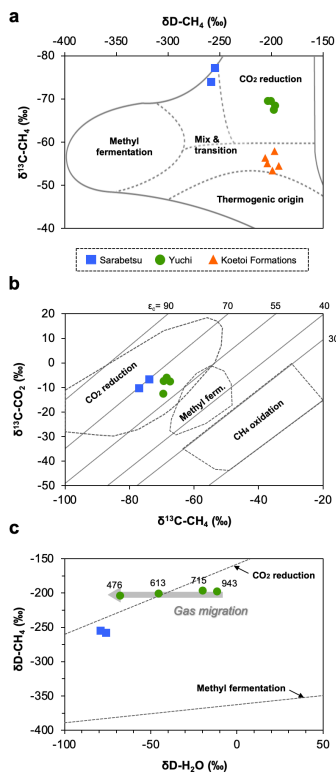
删除: approximately

删除: lack

删除: thermogenic

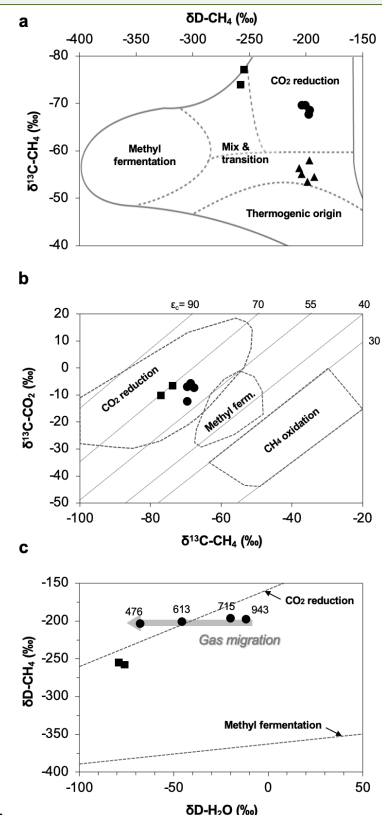
删除: produced at great depth

删除: samples implies that methanogenesis occurred within these formations. ...



340 **Figure 2.** Relationships between (a)  $\delta D$  and  $\delta^{13}C$  of methane, (b)  $\delta^{13}C$  of methane and  $\delta^{13}C$  of carbon dioxide, and (c)  $\delta D$  of  
 345 methane and  $\delta D$  of water for water samples from the upper Sarabetsu Formation (■) and the Yuchi Formation (●). The origins  
 of methane are estimated in each plot according to Whiticar (1999). In (a), data for water samples from the Koetoi Formation  
 (triangles) (Tamamura et al. 2014) are shown for comparison. The light gray diagonal lines in (b) indicate carbon isotopic  
 fractionation contours ( $\epsilon_c \approx \delta^{13}C-CO_2 - \delta^{13}C-CH_4$ ). In (c), the depths (mbs) of water samples from the Yuchi Formation are  
 indicated.

The TOC contents in sediment core samples from the Yuchi Formation ranged from less than 0.1% to more than 0.5%  
 (Fig. S4). Despite some dispersion associated with lithological changes, the TOC contents showed an overall increasing trend  
 with increasing depth ( $r = 0.77, p < 0.001$ ).



削除:

削除: squares

削除: circles

削除:

書式を変更: フォントの色: 黒

書式を変更: フォント: Symbol

削除: content

削除: ranges

削除: shows

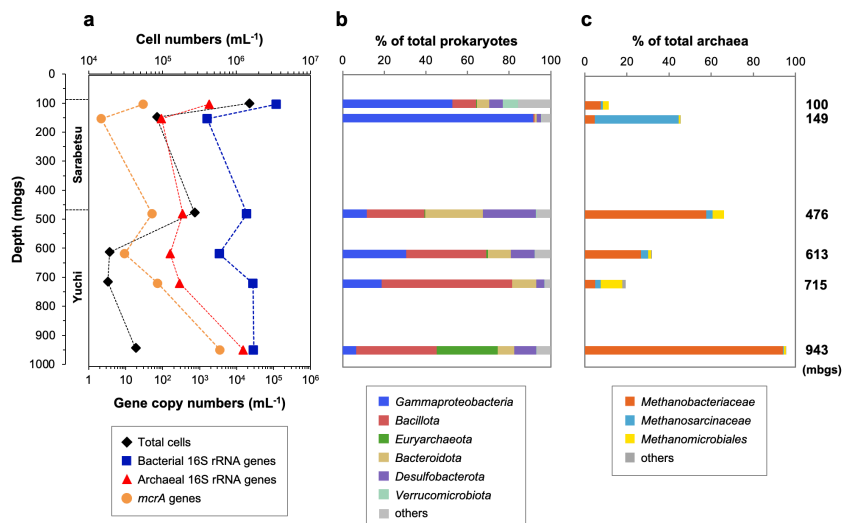
削除:



### 3.2 Enumeration of total microbial cells and of 16S rRNA and *mcrA* genes

360 The number of microbial cells in the water samples ranged from  $1.8 \times 10^4$  to  $1.5 \times 10^6$  cells  $\text{mL}^{-1}$  (Fig. 3a). The highest and lowest numbers were measured in the 100- and 715-mbgs samples, respectively, and the microbial cell densities in the studied aquifers are comparable to those reported in other deep aquifers ( $10^2$  to  $10^6$  cells  $\text{mL}^{-1}$ ) (Pedersen, 1993).

365 Bacterial and archaeal populations were measured by quantitative real-time PCR (Fig. 3a). The copy numbers of the bacterial 16S rRNA gene were  $10^3$ – $10^5$   $\text{mL}^{-1}$ , whereas those of archaea were  $10^2$ – $10^4$   $\text{mL}^{-1}$ . In the Yuchi Formation, the copy numbers of bacterial and archaeal genes were the highest in the deepest (943-mbgs) sample. The copy number of the *mcrA* gene, which is used to estimate methanogen populations, was also the highest in this sample at  $3.5 \times 10^3$  gene copies  $\text{mL}^{-1}$ , which is 2–3 orders of magnitude higher than the number of copies of the *mcrA* gene in the other samples.



370 **Figure 3.** Depth-related changes in (a) microbial populations and (b) prokaryotic and (c) methanogenic community compositions based on the 16S rRNA gene sequences in water samples.

### 3.3 Microbial community compositions in the water samples

375 The 454-pyrosequencing analysis of 16S rRNA genes was performed to examine the compositions of prokaryotic and methanogenic communities and their consistency with the *mcrA* gene sequencing analysis results, as described below. After quality filtering, the pyrosequencing reads yielded 14,304–43,532 reads per sample. The major taxonomic groups (>5% of the

削除: Copy

書式を変更: フォントの色: 黒

削除: ,

削除:

total reads in at least one sample) belonged to the following phyla or classes: *Gammaproteobacteria*, *Bacillota* (formerly *Firmicutes*), *Euryarchaeota*, *Bacteroidota*, *Desulfobacterota*, and *Verrucomicrobiota* (Fig. 3b). *Gammaproteobacteria* sequences were more abundant in the upper Sarabetsu Formation samples, whereas *Bacillota* and *Bacteroidota* were more abundant in the Yuchi Formation samples.

The sequences assigned to putative methanogens accounted for 0.2%–30% and 11%–95% of prokaryotic and archaeal 16S RNA gene sequences (Fig. 3c), respectively. The high proportion of methanogenic sequences in the 943-mbgs sample is consistent with the quantitative PCR results. Sequences assigned to hydrogenotrophic *Methanobacteriales* were commonly detected at all depths. In the 149-mbgs sample, high proportions of acetoclastic and/or methylotrophic methanogens of the genus *Methanosarcina* (*Methanosarcinales*) were detected.

Apart from the conventional methanogens mentioned above, recent studies indicate the potential of archaea outside the classification of Euryarchaeota to produce methane or break down nonmethane alkanes. Specifically, Methanomethylales, Nezharchaeales, Korarchaeia, and Methanodesulfokores have been found to possess methyl-S-CoM reductase, the central enzyme of methanogenesis, while Bathyarchaeota and Asgard possess alkyl-S-CoM reductase (Acr), which activates nonmethane alkanes (Mei et al., 2023). In the archaeal 16S RNA gene sequences of our samples, however, none of these potential methanogens or hydrocarbon-oxidizing archaea were identified.

#### 3.4 Methanogen diversity in the water samples based on the *mcrA* genes

A total of 64–69 clones of the *mcrA* gene per sample were grouped into 14 OTUs (Table 3). Similar to the 16S rRNA gene sequencing analysis results, methanogen diversity differed between the upper Sarabetsu and Yuchi Formation samples. Sequences related to acetoclastic *Methanosaeta* and hydrogenotrophic *Methanoregula* were abundant in the upper Sarabetsu Formation samples, whereas hydrogenotrophic *Methanobacterium* sequences were abundant in the Yuchi Formation samples. In the upper Sarabetsu Formation samples, *Candidatus* Methanoperedens, which oxidizes methane by coupling to nitrate reduction (Haroon et al., 2013), was also detected. Despite its high proportion, a shift in carbon isotope values toward the methane oxidation region on the  $\delta^{13}\text{C}\text{-CH}_4$  versus  $\delta^{13}\text{C}\text{-CO}_2$  plot (Whiticar, 1999) was not observed in those samples (Fig. 2b).

#### 3.5 Methanogen diversity in cultures

The 613- and 943-mbgs water samples from the Yuchi Formation aquifers were cultured with methanogenic substrates (i.e.,  $\text{H}_2/\text{CO}_2$  or acetate) under in situ salinity and temperature conditions to obtain culturable methanogens. Methane was produced from all samples. More than 82% (v/v) of the maximum theoretical yield of methane was obtained, indicating that the supplied methanogenic substrates were primarily used for methanogenesis.

In the acetate-amended cultures, *Methanosarcina* dominated, whereas *Methanoculleus* and *Methanobacterium* were detected in large proportions in the  $\text{H}_2/\text{CO}_2$ -amended cultures (Table 3). The sequences of these taxa were almost identical to those obtained directly from the original water samples, indicating that the predominant methanogens inhabiting the saline

削除:

書式を変更: フォント: 斜体(なし)

削除: towards

削除:

削除:

削除: .

削除: the

削除:

420 aquifers were successfully cultured. The diversity of the culturable methanogens was not clearly different between the 613-  
425 and 943-mbgs samples.

### 3.6 Effects of salinity and temperature on methanogenic activity

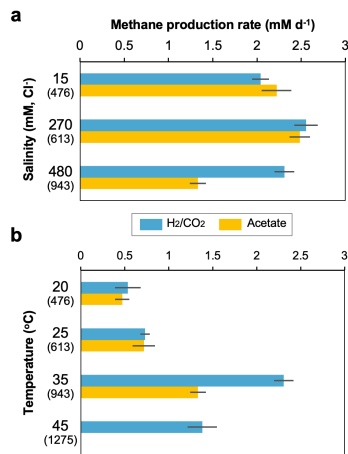
425 The methanogen cultures from the 943-mbgs water sample were subsequently cultured under different salinity and temperature  
430 conditions based on their depth profiles in the Yuchi Formation (Fig. 1b, d). In the H<sub>2</sub>/CO<sub>2</sub>-supplemented cultures, the methane  
production rate decreased slightly under the lowest salinity condition (i.e., 15 mM Cl<sup>-</sup>), whereas a more notable decrease was  
observed under the highest salinity condition (480 mM Cl<sup>-</sup>) in the acetate-supplemented cultures (Fig. 4a). Temperature  
changes more drastically affected methanogenic activity than salinity changes (Fig. 4b). In both H<sub>2</sub>/CO<sub>2</sub>- and acetate-  
supplemented cultures, methane production rates were the highest at 35 °C. At a temperature of 45 °C, which approximately  
corresponds to that at a depth of 1275 mbgs (assuming a thermal gradient of 2.92 °C per 100 m; Fig. 1d), methane production  
was observed only in the H<sub>2</sub>/CO<sub>2</sub>-amended culture.

删除:

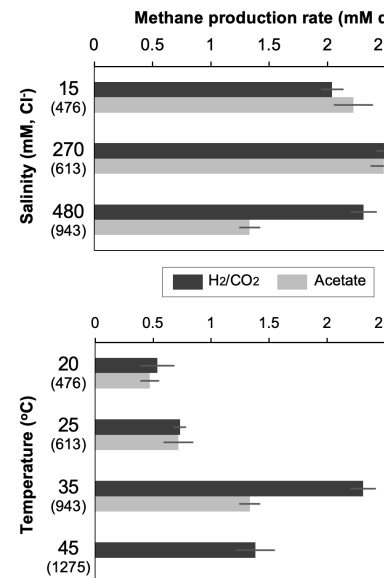
删除:

删除: production

删除: the



435 **Figure 4.** Effects of depth-related salinity (a) and temperature (b) changes on methane production rates in H<sub>2</sub>/CO<sub>2</sub>- and acetate-  
amended microcosms in the 943-mbgs water sample. The cultivation temperature for (a) was 35 °C, and the Cl<sup>-</sup> concentration  
in the culture medium for (b) was 480 mM. The values in parentheses are the depths (mbgs) of the saline aquifers corresponding  
to each culture condition.



删除:

### 3.7 The potential for syntrophic acetate oxidation (SAO) coupled with hydrogenotrophic methanogenesis

The SAO activity coupled with hydrogenotrophic methanogenesis (Zinder and Koch, 1984) in the 943-mbgs water sample was assessed by semicontinuous cultivation of SAO microorganisms fed a low concentration of acetate (Shigematsu et al., 2004) (Fig. S2a). After 10 months of cultivation, SAO activity was measured by using [2-<sup>13</sup>C]-acetate.

Methane was produced stoichiometrically from acetate in cultures supplemented with labeled and nonlabeled acetate (Fig. S2b). The values of  $\delta^{13}\text{C-DIC}$  increased from approximately -25‰ to 9‰ over time in the culture supplemented with [2-<sup>13</sup>C]-acetate, whereas no significant change was observed in the culture with nonlabeled acetate (Fig. S2c), clearly indicating SAO activity: in the acetoclastic methanogenic pathway, the methyl group of acetate is converted to methane but not to CO<sub>2</sub> (Ferry, 1993), whereas the methyl group of acetate is converted to CO<sub>2</sub> and subsequently to methane when SAO is coupled with hydrogenotrophic methanogenesis (Zinder and Koch, 1984).

#### 4 Discussion

This study examined microbial methane formation in relation to geochemical changes in deep sedimentary environments. Gas isotope analysis results suggested that methanogenesis occurred mostly via a carbonate reduction pathway in the Yuchi Formation. This finding is consistent with sequencing analysis results showing the predominance of hydrogenotrophic methanogens. In this formation, the isotopic ratio of hydrogen in water changed with depth and was coupled with a decrease in salinity due to diffusive mixing of brine with freshwater from the overlying formation (Ikawa et al., 2014). If substantial methanogenesis had occurred via the CO<sub>2</sub> reduction pathway after this dilution, the  $\delta\text{D-CH}_4$  value would have changed along with the  $\delta\text{D-H}_2\text{O}$  value and become distinct from the value of the deepest 943-mbgs sample, that is, the least diluted brine. This change would have occurred because all hydrogen atoms in methane produced via the CO<sub>2</sub> reduction pathway are derived from ambient water (Daniels et al., 1980). However, the results showed almost no change in  $\delta\text{D-CH}_4$  compared with  $\delta\text{D-H}_2\text{O}$ , suggesting that in situ methanogenesis in the shallow part of this formation does not contribute significantly to methane deposits overall and that methane produced in the deeper layers of the Yuchi Formation migrated upward in association with the diffusive mixing of brine with freshwater (Fig. 2c).

This interpretation is supported by the experimental results. A distinctly high methanogen population, composed primarily of hydrogenotrophic methanogens, was observed in the deepest brine sample. In addition, hydrogenotrophic methanogenesis was estimated to proceed faster in deeper aquifers in the Yuchi Formation, where salinity and temperature are higher. The TOC content of the sediment core samples from this formation increased with depth, and the sediments adjacent to the deepest aquifer contained 2 to 3 times as much TOC as those adjacent to other, shallower aquifers (Fig. S4). Similar to our results, the population of microorganisms, including methanogens represented by their lipid biomarkers, locally increases with increasing TOC content in deep marine sediments (Cragg et al., 1996; Oba et al., 2015). Previous studies have indicated that low-permeability sediments are rich in organic materials and that their fermentation products, such as acetate, diffuse into adjacent, more permeable aquifers, where they are consumed by microorganisms (McMahon and Chapelle, 1991; Krumholz et al., 1997). Previous laboratory heating experiments simulating the burial of marine sediments have shown an increase in acetate, which may sustain the deep seafloor biosphere (Wellsbury et al., 1997). Indeed, the porewater acetate concentration in deep

削除: semi-continuous

削除: with

削除: non-labeled

削除: Values

削除: non-labeled

削除:

削除: the

書式を変更: フォント:斜体(なし)

削除:

削除: remarkably

削除: methanogenesis

書式を変更: フォントの色: 黒

削除: potentially

490 [subseafloor sediments increases with depth, which stimulates potential methanogenic activities \(Heuer et al., 2020; Beulig et al., 2022\)](#). Collectively, these data suggest that with increasing depth, an increased organic carbon content provides microorganisms with more energy and carbon sources, and that the increased temperature accelerates the biodegradation of sedimentary organic matter and methanogenesis; as a result, the deepest aquifers in the Yuchi Formation function as sources of microbial methane. Acetate is considered a key intermediate product, but as described above, acetoclastic methanogens constitute a minor proportion of the methanogens in the Yuchi Formation, and in our experiments under [high salinity conditions](#), corresponding to that of the deepest sample, methanogenic activity from acetate decreased. We further demonstrate the [SAO activity](#) coupled with hydrogenotrophic methanogenesis to convert acetate to methane in the [sample from the deep part of this formation](#). [A previous study suggested the potential for SAO with methanogenesis in deep subseafloor sediments at high temperatures \(Beulig et al., 2022\)](#). Investigating the diversity of microorganisms involved in SAO in deep subsurface environments is among the targets for future [studies](#).

500 Our findings offer insight into microbial processes in the global carbon cycle over geological timescales and provide important reference data for geomicrobiological studies of deep subsurface environments that are enriched in microbial methane.

505 *Data Availability.* DNA sequencing data are available at GenBank, as described in the [Materials](#) and Methods section. Other datasets generated during the current study are available from the corresponding author [upon](#) reasonable request.

*Competing Interests.* The authors have no relevant financial or [nonfinancial](#) interests to disclose.

510 *Author Contributions.* All authors contributed to the study conception and design. Taiki Katayama, Reo Ikawa, and Masaru Koshigai collected the samples. Reo Ikawa and Masaru Koshigai analyzed the water and sediment geochemistry. Susumu Sakata analyzed the gas geochemistry. Taiki Katayama performed the cultivation experiments and the DNA sequencing analysis. All [the](#) authors [have](#) read and approved the final manuscript.

515 *Acknowledgments.* This study was carried out as a part of [the](#) R&D supporting program titled “Development of enhancing the evaluation technology for fresh-salt water interface in the coastal region” (2012 FY) under the contract with [the](#) Ministry of Economy, Trade and Industry (METI). This study was also financially supported in part by [the](#) Japan Society for the Promotion of Science KAKENHI grant numbers JP17K15183 and JP18H05295. We thank Hanako Mochimaru, Chiwaka Miyako, and Fumie Nozawa for assistance in the sample collection, sequencing analysis, and cultivation experiments. Thanks are further extended to Atsunao Marui for managing the borehole drilling project and to Yoichi Kamagata for valuable comments that  
520 improved our manuscript.

删除: ,

删除: a

删除:

删除: condition

删除: potential for

删除: study

删除: Material

删除: on

删除: non-financial

530 **References**

- [Beulig, F., Schubert, F., Adhikari, R. R., Glombitza, C., Heuer, V. B., Hinrichs, K. U., Homola, K. L., Inagaki, F., Jørgensen, B. B., Kallmeyer, J., Krause, S., J. E. Morono, Y., Sauvage, J., Spivack, A. J., and Treude, T.: Rapid metabolism fosters microbial survival in the deep, hot seafloor biosphere. \*Nat Commun\*, 13, 312, \[10.1038/s41467-021-27802-7\]\(https://doi.org/10.1038/s41467-021-27802-7\), 2022.](#)
- Cragg, B. A., Parkes, R. J., Fry, J. C., Weightman, A. J., Rochelle, P. A., and Maxwell, J. R.: Bacterial populations and processes in sediments containing gas hydrates (ODP Leg 146: Cascadia Margin). *Earth Planet. Sc. Lett.*, 139, 497-507, [https://doi.org/10.1016/0012-821x\(95\)00246-9](https://doi.org/10.1016/0012-821x(95)00246-9), 1996.
- Daniels, L., Fulton, G., Spencer, R. W., and Ormejohnson, W. H.: Origin of hydrogen in methane produced by *Methanobacterium thermoautotrophicum*. *J. Bacteriol.*, 141, 694-698, <https://doi.org/10.1128/jb.141.2.694-698.1980>, 1980.
- Ferry, J. G.: Fermentation of acetate, in: *Methanogenesis*, edited by: Ferry, J. G., Chapman & Hall Microbiology Series, Springer, U.S.A., 304-334, doi: 10.1007/978-1-4615-2391-8\_7, 1993.
- Fredrickson, J. K., McKinley, J. P., Bjornstad, B. N., Long, P. E., Ringelberg, D. B., White, D. C., Krumholz, L. R., Suflita, J. M., Colwell, F. S., Lehman, R. M., Phelps, T. J., and Onstott, T. C.: Pore-size constraints on the activity and survival of subsurface bacteria in a late Cretaceous shale-sandstone sequence, northwestern New Mexico. *Geomicrobiol. J.*, 14, 183-202, <https://doi.org/10.1080/01490459709378043>, 1997.
- 545 Haroon, M. F., Hu, S., Shi, Y., Imelfort, M., Keller, J., Hugenholtz, P., Yuan, Z., and Tyson, G. W.: Anaerobic oxidation of methane coupled to nitrate reduction in a novel archaeal lineage. *Nature*, 500, 567-570, <https://doi.org/10.1038/nature12375>, 2013.
- [Heuer, V. B., Inagaki, F., Morono, Y., Kubo, Y., Spivack, A. J., Viehweger, B., Treude, T., Beulig, F., Schubert, F., Tonai, S., Bowden, S. A., Cramm, M., Henkel, S., Hirose, T., Homola, K., Hoshino, T., Ijiri, A., Imachi, H., Kamiya, N., Kaneko, M., Lagostina, L., Manners, H., McClelland, H.-L., Metcalfe, K., Okutsu, N., Pan, D., Raudsepp, M. J., Sauvage, J., Tsang, M.-Y., Wang, D. T., Whitaker, E., Yamamoto, Y., Yang, K., Maeda, L., Adhikari, R. R., Glombitza, C., Hamada, Y., Kallmeyer, J., Wendt, J., Wörmer, L., Yamada, Y., Kinoshita, M., and Hinrichs, K.-U.: Temperature limits to deep seafloor life in the Nankai Trough subduction zone. \*Science\*, 370, 1230-1234, \[10.1126/science.abd7934\]\(https://doi.org/10.1126/science.abd7934\), 2020.](#)
- Ikawa, R., Machida, I., Koshigai, M., Nishizaki, S., and Marui, A.: Coastal aquifer system in late Pleistocene to Holocene deposits at Horonobe in Hokkaido, Japan. *Hydrogeol. J.*, 22, 987-1002, <https://doi.org/10.1007/s10040-014-1106-4>, 2014.
- Katayama, T. and Kamagata, Y.: Cultivation of methanogens, in: *Isolation and Cultivation (Hydrocarbon and Lipid Microbiology Protocols)*, edited by: McGenity, T. J., Timmis, K. N., Nogales, B., Springer Berlin, Heidelberg, 177-195, <https://doi.org/10.1007/978-3-662-45179-3>, 2018
- Katayama, T., Nobu, M.K., Kusada, H., Meng, X.Y., Hosogi, N., Uematsu, K., Yoshioka, H., Kamagata, Y., and Tamaki, H.: Isolation of a member of the candidate phylum 'Atribacteria' reveals a unique cell membrane structure. *Nat. Commun.*, 11, 6381, <https://doi.org/10.1038/s41467-020-20149-5>, 2020.
- 550

移動 (挿入) [1]

移動 (挿入) [2]

削除: ↵

- Katayama, T., Yoshioka, H., Kaneko, M., Amo, M., Fujii, T., Takahashi, H.A., Yoshida, S., and Sakata, S.: Cultivation and biogeochemical analyses reveal insights into methanogenesis in deep subseafloor sediment at a biogenic gas hydrate site. *ISME J.*, 16, 1464-1472, <https://doi.org/10.1038/s41396-021-01175-7>, 2022.
- Katayama, T., Yoshioka, H., Muramoto, Y., Usami, J., Fujiwara, K., Yoshida, S., Kamagata, Y., and Sakata, S. Physicochemical impacts associated with natural gas development on methanogenesis in deep sand aquifers. *ISME J.*, 9, 436-446, <https://doi.org/10.1038/ismej.2014.140>, 2015.
- Katoh, K. and Standley, D. M.: MAFFT multiple sequence alignment software version 7: improvements in performance and usability. *Mol. Biol. Evol.*, 30, 772-780, <https://doi.org/10.1093/molbev/mst010>, 2013
- ~~Kotelnikova, S.: Microbial production and oxidation of methane in deep subsurface. *Earth-Sci. Rev.*, 58, 367-395, [https://doi.org/Pii S0012-8252\(01\)00082-4](https://doi.org/Pii%20S0012-8252(01)00082-4), 2002~~
- Krumholz, L. R., McKinley, J. P., Ulrich, F. A., and Suflita, J. M.: Confined subsurface microbial communities in Cretaceous rock. *Nature*, 386, 64-66, [https://doi.org/Doi 10.1038/386064a0](https://doi.org/Doi%2010.1038/386064a0), 1997.
- 575 ~~Liu, L.-Y., Xie, G.-J., Ding, J., Liu, B.-F., Xing, D.-F., Ren, N.-Q., and Wang, Q.: Microbial methane emissions from the non-methanogenesis processes: A critical review. *Science of The Total Environment*, 806, 151362, <https://doi.org/10.1016/j.scitotenv.2021.151362>, 2022.~~
- Lovley, D. R. and Chapelle, F. H.: Deep subsurface microbial processes. *Rev. Geophys.*, 33, 365-381, [https://doi.org/Doi 10.1029/95rg01305](https://doi.org/Doi%2010.1029/95rg01305), 1995.
- 580 Luton, P.E., Wayne, J.M., Sharp, R.J., and Riley, P.W.: The mcrA gene as an alternative to 16S rRNA in the phylogenetic analysis of methanogen populations in landfill. *Microbiol.*, 148, 3521-3530, <https://doi.org/10.1099/00221287-148-11-3521>, 2002.
- ~~Mayumi, D., Mochimaru, H., Tamaki, H., Yamamoto, K., Yoshioka, H., Suzuki, Y., Kamagata, Y., and Sakata, S.: Methane production from coal by a single methanogen. *Science*, 354, 222-225, doi:10.1126/science.aaf8821, 2016.~~
- 585 ~~McMahon, P. B. and Chapelle, F. H.: Microbial production of organic acids in aquitard sediments and its role in aquifer geochemistry. *Nature*, 349, 233-235, [https://doi.org/Doi 10.1038/349233a0](https://doi.org/Doi%2010.1038/349233a0), 1991.~~
- McMahon, S. and Parnell, J.: Weighing the deep continental biosphere. *FEMS Microbiol. Ecol.* 87, 113-120, <https://doi.org/10.1111/1574-6941.12196>, 2014.
- ~~Mei, R., Kaneko, M., Imachi, H., and Nobu, M. K.: The origin and evolution of methanogenesis and Archaea are intertwined. *PNAS Nexus*, 2, 10.1093/pnasnexus/pgad023, 2023.~~
- 590 ~~Mesle, M., Dromart, G., and Oger, P.: Microbial methanogenesis in subsurface oil and coal. *Res. Microbiol.*, 164, 959-872, <https://doi.org/10.1016/j.resmic.2013.07.004>, 2013.~~
- Oba, M., Sakata, S., and Fujii, T.: Archaeal polar lipids in subseafloor sediments from the Nankai Trough: Implications for the distribution of methanogens in the deep marine subsurface. *Org. Geochem.*, 78, 153-160, <https://doi.org/10.1016/j.orggeochem.2014.11.006>, 2015.

上へ移動【1】: J.

削除: Katz, B. J.: Microbial processes and natural gas accumulations. *Open*

削除: *Geol.*, 5, 75-83, DOI: 10.2174/1874262901105010075, 2011

削除: Magnabosco, C., Lin, L.H., Dong, H., Bomberg, M., Ghiorse, W., Stan-Lotter, H., Pedersen, K., Kieft, T.L., van Heerden,

上へ移動【2】: E.,

削除: and Onstott, T.C.: The biomass and biodiversity of the continental subsurface. *Nat. Geosci.*, 11, 707-717, <https://doi.org/10.1038/s41561-018-0221-6>, 2018.

- Pedersen, K.: The deep subterranean giosphere. *Earth-Sci. Rev.*, 34, 243-260, [https://doi.org/Doi 10.1016/0012-8252\(93\)90058-F](https://doi.org/Doi 10.1016/0012-8252(93)90058-F), 1993.
- Pruesse, E., Quast, C., Knittel, K., Fuchs, B.M., Ludwig, W., Peplies, J., and Glockner, F.O.: SILVA: a comprehensive online resource for quality checked and aligned ribosomal RNA sequence data compatible with ARB. *Nucleic Acids Res.* 35, 7188-7196, <https://doi.org/10.1093/nar/gkm864>, 2007.
- Schloss, P.D., Westcott, S.L., Ryabin, T., Hall, J.R., Hartmann, M., Hollister, E.B., Lesniewski, R.A., Oakley, B.B., Parks, D.H., Robinson, C.J., Sahl, J.W., Stres, B., Thallinger, G.G., Van Horn, D.J., and Weber, C.F.: Introducing mothur: open-source, platform-independent, community-supported software for describing and comparing microbial communities. *Appl. Environ. Microbiol.*, 75, 7537-7541, <https://doi.org/10.1128/AEM.01541-09>, 2009.
- Shigematsu, T., Tang, Y.Q., Kobayashi, T., Kawaguchi, H., Morimura, S., and Kida, K.: Effect of dilution rate on metabolic pathway shift between acetitlastic and nonacetitlastic methanogenesis in chemostat cultivation. *Appl. Environ. Microbiol.*, 70, 4048-4052, <https://doi.org/Doi 10.1128/Aem.70.7.4048-4052.2004>, 2004.
- Tamamura, S., Akatsuka, M., Ikawa, R., Koshigai, M., Shiimizu, S., Ueno, A., Ohmi, Y., Kaneko, K., Igarashi, T., and Marui, A.: Origin of methane dissolved in formation waters in the Koetoi Formation through the alluvium in northwestern part of Hokkaido, Japan. *Geochemistry*, 48, 39-50, <https://doi.org/10.14934/chikyukagaku.48.39>, 2014.
- Tani, H., Miyata, R., Ichikawa, K., Morishita, S., Kurata, S., Nakamura, K., Tsuneda, S., Sekiguchi, Y., and Noda, N.: Universal quenching probe system: flexible, specific, and cost-effective real-time polymerase chain reaction method. *Anal. Chem.*, 81,5678-5685, <https://doi.org/Doi 10.1021/Ac900414u>, 2009.
- Wellsbury, P., Goodman, K., Barth, T., Cragg, B.A., Barnes, S.P., and Parkes, R.J.: Deep marine biosphere fuelled by increasing organic matter availability during burial and heating. *Nature*, 388, 573-576, <https://doi.org/10.1038/41544>, 1997.
- Whiticar, M. J.: Carbon and hydrogen isotope systematics of bacterial formation and oxidation of methane. *Chem. Geol.* 161, 291-314, [https://doi.org/Doi 10.1016/S0009-2541\(99\)00092-3](https://doi.org/Doi 10.1016/S0009-2541(99)00092-3), 1999.
- Zhang, S., Shuai, Y., Huang, L., Wang, L., Su, J., Huanh, H., Ma, D., and Li, M.: Timing of biogenic gas formation in the Qaidam Basin, NW China. *Chem. Geol.* 352, 70-80, <https://doi.org/Doi 10.1016/j-chemgeo.2013.06.001>, 2013.
- Zhou, Z., Zhang, C. J., Liu, P. F., Fu, L., Laso-Pérez, R., Yang, L., Bai, L. P., Li, J., Yang, M., Lin, J. Z., Wang, W. D., Wegener, G., Li, M., and Cheng, L.: Non-syntrophic methanogenic hydrocarbon degradation by an archaeal species. *Nature*, 601, 257-262, [10.1038/s41586-021-04235-2](https://doi.org/10.1038/s41586-021-04235-2), 2022.
- Zinder, S. and Koch, M.: Non-aceticlastic methanogenesis from acetate: acetate oxidation by a thermophilic syntrophic coculture. *Arch. Microbiol.* 138, 263-272, <https://doi.org/10.1007/BF00402133>, 1984.

635



**Table 1.** Geochemical characteristics of the water samples.

Depth (mbgs)	pH	ORP	Temp	HCO <sub>3</sub> <sup>-</sup>	Cl <sup>-</sup>	NO <sub>3</sub> <sup>-</sup>	Br <sup>-</sup>	SO <sub>4</sub> <sup>2-</sup>	PO <sub>4</sub> <sup>3-</sup>	Na <sup>+</sup>	NH <sub>4</sub> <sup>+</sup>	K <sup>+</sup>	Mg <sup>2+</sup>	Ca <sup>2+</sup>	Fe <sup>2+</sup>	DOC	Ace.	δD
		(mV)	(°C)	(mg L <sup>-1</sup> )	(mg L <sup>-1</sup> )	(mg L <sup>-1</sup> )	(mg L <sup>-1</sup> )	(mg L <sup>-1</sup> )	(mg L <sup>-1</sup> )	(mg L <sup>-1</sup> )	(mg L <sup>-1</sup> )	(mg L <sup>-1</sup> )	(mg L <sup>-1</sup> )	(mg L <sup>-1</sup> )	(mg L <sup>-1</sup> )	(mg L <sup>-1</sup> )	(mg L <sup>-1</sup> )	(‰ vs. VSMOW)
100	7.2	-200	10.6	453	165	1.4	1.4	0.6	bdl	146	4.3	22	38	37	ndt	7.5	0.2	-79
149	7.3	-210	12.1	395	306	bdl	2.8	0.1	bdl	160	15	20	66	50	ndt	5.2	0.029	-76
476	8	-490	22.2	637	1750	bdl	17	bdl	1.5	1030	14	58	84	54	0.6	36	2.2	-68
613	7.6	-290	25.6	2150	9500	bdl	96	bdl	6.4	5640	79	230	270	89	1.4	85	0.63	-46
715	7	-380	28.3	2980	15600	bdl	170	bdl	7.5	9830	110	390	420	79	ndt	170	0.12	-20
943	8.1	-450	35.4	3610	17100	bdl	140	bdl	bdl	11100	210	440	310	100	1.6	220	16	-12

Abbreviations: Ace., acetate; bdl, below the detection limit; DOC, dissolved organic carbon; ORP, oxidation–reduction potential; ndt, not determined; Temp, temperature.

書式変更: 左: 10 mm, 右: 23.6 mm, 上: 16.5 mm, 下: 16.5 mm, 幅: 240 mm, 高さ: 210 mm

挿入されたセル

挿入されたセル

挿入されたセル

挿入されたセル

挿入されたセル

挿入されたセル

挿入されたセル

挿入されたセル

挿入されたセル

書式を変更: フォント: 5 pt

移動 (挿入) [3]

移動 (挿入) [4]

**Table 2.** Geochemical characteristics of the dissolved gas samples.

Depth (mbgs)	Dissolved gas composition (%)				Isotopic ratios (‰)		
	N <sub>2</sub>	CO <sub>2</sub>	CH <sub>4</sub>	C <sub>2</sub> H <sub>6</sub>	$\delta^{13}\text{C}$ (vs. VPDB)		$\delta\text{D}$ (vs. VSMOW)
					CO <sub>2</sub>	CH <sub>4</sub>	CH <sub>4</sub>
100	21.40	1.75	76.86	0	-10.3	-77.1	-255
149	16.65	2.76	80.58	0	-6.7	-73.9	-258
476	8.82	0.82	90.35	0	-12.5	-69.5	-203
613	4.23	4.11	91.67	0	-7.3	-69.5	-201
715	0.72	6.71	92.55	0.02	-6.0	-68.5	-196
943	1.75	9.84	88.37	0.03	-7.4	-67.5	-198

- 書式を変更 ... [1]
- 書式変更 ... [2]
- 削除: Depth (mbgs) ... [3]
- 上へ移動 [3]: ←
- 削除: Acetate; bdl, below detection limit; DOC, Dissolved or ... [4]
- 上へ移動 [4]: ..... 改ページ
- 削除: ←
- 書式を変更 ... [5]
- 削除: CH<sub>4</sub> ... [6]
- 書式変更 ... [6]
- 削除: CO<sub>2</sub> ... [7]
- 書式変更 ... [7]
- 削除:  $\delta\text{D}$  ... [8]
- 書式変更 ... [8]
- 削除:  $\delta^{13}\text{C}$  ... [9]
- 書式を変更 ... [9]
- 削除:  $\delta^{13}\text{C}$  ... [10]
- 削除: 4 ... [10]
- 書式変更 ... [10]
- 削除: 255 ... [11]
- 削除: 10.3 ... [11]
- 書式変更 ... [11]
- 削除: 258 ... [12]
- 削除: 6.7 ... [12]
- 書式変更 ... [12]
- 削除: 203 ... [13]
- 削除: 12.5 ... [13]
- 書式変更 ... [13]
- 削除: 201 ... [14]
- 削除: 7.3 ... [14]
- 書式変更 ... [14]
- 削除: 196 ... [15]
- 削除: 6.0 ... [15]
- 削除: 198 ... [15]
- 削除: 7.4 ... [15]
- 書式変更 ... [15]
- 書式を変更 ... [16]
- 書式を変更 ... [17]

**Table 3.** Methanogen diversity based on the *mcrA* gene in the original water and culture samples

Representative clone ID in OTU	Accession no.	Related species	Identity (%)	Original water samples				Culture samples					
				Sarabetsu		Yuchi		H <sub>2</sub> /CO <sub>2</sub>		Acetate			
				100	149	476	613	715	943	613	943	613	943
D3mf21	LC214931	<i>Methanosarcina mazei</i>	97.8	2.9	2.9								
D14mf19	LC214911	<i>Methanosarcina subterranea</i>	98.6			4.5	12.7						
D16Amf09	LC214912	<i>Methanosarcina subterranea</i>	99.3						6.1		90.0	86.8	
D13mf35	LC214921	<i>Methanobolbus psychrophilus</i>	99.3			7.5	3.2	1.4					
D2mf17	LC214928	<i>Candidatus Methanoperedens nitroreducens</i>	83.5	71.0	18.8								
D3mf15	LC214933	<i>Methanosaepta harundinacea</i>	95.5	11.6	20.3								
D15mf27	LC214924	<i>Methanoregula formicica</i>	84.9			1.6	95.2						
D3mf09	LC214929	<i>Methanoregula boonei</i>	86.4	14.5	46.4								
D14mf27	LC214922	<i>Methanolinea mesophila</i>	92.9			14.9	1.6						
D3mf29	LC214934	<i>Methanospirillum psychrodurum</i>	100		4.3								
D3mf07	LC214932	<i>Methanocalculus alkaliphilus</i>	95.1		4.3								
D16mf37	LC214927	<i>Methanoculleus sediminis</i>	100			11.1	9.9						
D14Hmf08	LC214914	<i>Methanoculleus sediminis</i>	100						36.4	27.0	5.0	2.6	
D16Hmf21	LC214917	<i>Methanoculleus bourgensis</i>	92.9							13.5			
D14Hmf25	LC214915	<i>Methanoculleus horonobensis</i>	100						48.5	43.2		5.3	
D16mf23	LC214925	<i>Methanoculleus horonobensis</i>	99.3			4.8	12.7						
D3mf17	LC214930	<i>Methanobacterium alkalithermotolerans</i>	100		2.9								
D16mf17	LC214926	<i>Methanobacterium alkalithermotolerans</i>	100			73.1	65.1	4.8	76.1				
D3Amf10	LC214935	<i>Methanobacterium alkalithermotolerans</i>	100							9.1	16.2	5.0	5.3

- 削除: [21]
- 書式を変更 [24]
- 書式を変更 [22]
- 書式を変更 [23]
- 書式を変更 [25]
- 書式を変更 [18]
- 書式を変更 [20]
- 書式を変更 [19]
- 書式を変更 [30]
- 書式を変更 [32]
- 書式を変更 [33]
- 書式を変更 [34]
- 書式を変更 [35]
- 書式を変更 [36]
- 書式を変更 [31]
- 書式を変更 [26]
- 書式を変更 [28]
- 書式を変更 [27]
- 書式を変更 [29]
- 書式を変更 [41]
- 書式を変更 [43]
- 書式を変更 [44]
- 書式を変更 [45]
- 書式を変更 [42]
- 書式を変更 [46]
- 書式を変更 [37]
- 書式を変更 [39]
- 書式を変更 [38]
- 書式を変更 [40]
- 書式を変更 [47]
- 書式を変更 [49]
- 書式を変更 [48]
- 書式を変更 [50]
- 書式を変更 [51]
- 書式を変更 [52]
- 書式を変更 [54]
- 書式を変更 [55]
- 書式を変更 [56]
- 書式を変更 [57]
- 書式を変更 [58]
- 書式を変更 [59]
- 書式を変更 [60]
- 書式を変更 [64]
- 書式を変更 [61]
- 書式を変更 [65]
- 書式を変更 [62]

ページ 18: [1] 書式を変更 作成者

フォント: 9 pt, フォントの色: 自動

ページ 18: [2] 書式変更 作成者

なし

ページ 18: [3] 削除 作成者

ページ 18: [4] 削除 作成者

ページ 18: [5] 書式を変更 作成者

英語 (米国)

ページ 18: [5] 書式を変更 作成者

英語 (米国)

ページ 18: [6] 書式変更 作成者

行間: 1.5 行

ページ 18: [7] 書式変更 作成者

行間: 1.5 行

ページ 18: [8] 書式変更 作成者

行間: 1.5 行

ページ 18: [9] 書式を変更 作成者

英語 (米国)

ページ 18: [9] 書式を変更 作成者

英語 (米国)

ページ 18: [10] 書式変更 作成者

行間: 1.5 行

ページ 18: [11] 書式変更 作成者

行間: 1.5 行

ページ 18: [12] 書式変更 作成者

行間: 1.5 行

ページ 18: [13] 書式変更 作成者

行間: 1.5 行

ページ 18: [14] 書式変更 作成者

行間: 1.5 行

ページ 18: [15] 書式変更 作成者

行間: 1.5 行

ページ 18: [16] 書式を変更 作成者

英語 (米国)

ページ 18: [16] 書式を変更 作成者

英語 (米国)

ページ 18: [17] 書式を変更 作成者

英語 (米国)

ページ 18: [17] 書式を変更 作成者

英語 (米国)

ページ 19: [18] 書式を変更 作成者

フォント: Times New Roman, 10 pt, フォントの色: テキスト 1

ページ 19: [19] 書式変更 作成者

両端揃え, 行間: 1.5 行

ページ 19: [20] 書式を変更 作成者

フォントの色: テキスト 1

ページ 19: [21] 書式を変更 作成者

フォント: 7 pt, フォントの色: テキスト 1

ページ 19: [22] 書式変更 作成者

行間: 1.5 行

ページ 19: [23] 書式変更 作成者

両端揃え, 行間: 1.5 行

ページ 19: [24] 書式を変更 作成者

フォント: 7 pt, フォントの色: テキスト 1

ページ 19: [25] 書式変更 作成者

行間: 1.5 行

ページ 19: [26] 書式を変更 作成者

フォント: 7 pt, フォントの色: テキスト 1

ページ 19: [27] 書式変更 作成者

行間: 1.5 行

ページ 19: [28] 書式を変更 作成者

フォントの色: テキスト 1

ページ 19: [29] 書式変更 作成者

両端揃え, 行間: 1.5 行

ページ 19: [30] 書式を変更 作成者

フォント: 7 pt, フォントの色: テキスト 1

ページ 19: [31] 書式変更 作成者

行間: 1.5 行

ページ 19: [32] 書式を変更 作成者

フォント: Arial, 7 pt, フォントの色: テキスト 1, 英語 (米国)

ページ 19: [32] 書式を変更 作成者

フォント: Arial, 7 pt, フォントの色: テキスト 1, 英語 (米国)

ページ 19: [33] 書式を変更 作成者

フォント: 7 pt, フォントの色: テキスト 1

ページ 19: [34] 書式を変更 作成者

フォント: 5.5 pt, フォントの色: テキスト 1



ページ 19: [34] 書式を変更 作成者

フォント : 5.5 pt, フォントの色 : テキスト 1

ページ 19: [34] 書式を変更 作成者

フォント : 5.5 pt, フォントの色 : テキスト 1

ページ 19: [34] 書式を変更 作成者

フォント : 5.5 pt, フォントの色 : テキスト 1

ページ 19: [35] 書式を変更 作成者

フォント : Arial, 7 pt, フォントの色 : テキスト 1, 英語 (米国)

ページ 19: [35] 書式を変更 作成者

フォント : Arial, 7 pt, フォントの色 : テキスト 1, 英語 (米国)

ページ 19: [36] 書式を変更 作成者

フォント : 7 pt, フォントの色 : テキスト 1

ページ 19: [37] 書式を変更 作成者

フォント : 7 pt, フォントの色 : テキスト 1

ページ 19: [38] 書式変更 作成者

行間 : 1.5 行

ページ 19: [39] 書式を変更 作成者

フォントの色: テキスト 1

ページ 19: [40] 書式変更 作成者

両端揃え, 行間: 1.5 行

ページ 19: [41] 書式を変更 作成者

フォント: 7 pt, フォントの色: テキスト 1

ページ 19: [42] 書式変更 作成者

行間: 1.5 行

ページ 19: [43] 書式を変更 作成者

フォント: Arial, 7 pt, フォントの色: テキスト 1, 英語 (米国)

ページ 19: [43] 書式を変更 作成者

フォント: Arial, 7 pt, フォントの色: テキスト 1, 英語 (米国)

ページ 19: [44] 書式を変更 作成者

フォント: 7 pt, フォントの色: テキスト 1

ページ 19: [45] 書式を変更 作成者

フォント : Arial, 7 pt, フォントの色 : テキスト 1, 英語 (米国)

ページ 19: [45] 書式を変更 作成者

フォント : Arial, 7 pt, フォントの色 : テキスト 1, 英語 (米国)

ページ 19: [46] 書式を変更 作成者

フォント : 7 pt, フォントの色 : テキスト 1

ページ 19: [47] 書式を変更 作成者

フォント : 7 pt, フォントの色 : テキスト 1

ページ 19: [48] 書式変更 作成者

行間 : 1.5 行

ページ 19: [49] 書式を変更 作成者

フォント : Arial, 7 pt, フォントの色 : テキスト 1, 英語 (米国)

ページ 19: [49] 書式を変更 作成者

フォント : Arial, 7 pt, フォントの色 : テキスト 1, 英語 (米国)

ページ 19: [50] 書式を変更 作成者

フォント : 7 pt, フォントの色 : テキスト 1

ページ 19: [51] 書式を変更 作成者

フォント : Arial, 7 pt, フォントの色 : テキスト 1, 英語 (米国)

ページ 19: [52] 書式変更 作成者

行間 : 1.5 行

ページ 19: [53] 書式を変更 作成者

フォント : Arial, 7 pt, フォントの色 : テキスト 1

ページ 19: [54] 書式を変更 作成者

フォント : Arial, 7 pt, フォントの色 : テキスト 1

ページ 19: [55] 書式変更 作成者

行間 : 1.5 行

ページ 19: [56] 書式を変更 作成者

フォント : 7 pt, フォントの色 : テキスト 1

ページ 19: [57] 書式変更 作成者

行間 : 1.5 行

ページ 19: [58] 書式を変更 作成者

フォントの色 : テキスト 1

ページ 19: [59] 書式変更 作成者

両端揃え, 行間: 1.5 行

ページ 19: [60] 書式を変更 作成者

フォント: 7 pt, フォントの色: テキスト 1

ページ 19: [61] 書式変更 作成者

行間: 1.5 行

ページ 19: [62] 書式を変更 作成者

フォントの色: テキスト 1

ページ 19: [63] 書式変更 作成者

両端揃え, 行間: 1.5 行

ページ 19: [64] 書式を変更 作成者

フォント: 7 pt, フォントの色: テキスト 1

ページ 19: [65] 書式変更 作成者

行間: 1.5 行

ページ 19: [66] 書式を変更 作成者

フォントの色: テキスト 1

ページ 19: [67] 書式変更 作成者

両端揃え, 行間: 1.5 行

ページ 19: [68] 書式を変更 作成者

フォント: 7 pt, フォントの色: テキスト 1

ページ 19: [69] 書式変更 作成者

行間: 1.5 行

ページ 19: [70] 書式を変更 作成者

フォントの色: テキスト 1

ページ 19: [71] 書式変更 作成者

両端揃え, 行間: 1.5 行

ページ 19: [72] 書式を変更 作成者

フォント: 7 pt, フォントの色: テキスト 1

ページ 19: [73] 書式変更 作成者

行間: 1.5 行

ページ 19: [74] 書式を変更 作成者

フォントの色: テキスト 1

ページ 19: [75] 書式変更 作成者

両端揃え, 行間: 1.5 行

ページ 19: [76] 書式を変更 作成者

フォント: 7 pt, フォントの色: テキスト 1

ページ 19: [77] 書式変更 作成者

行間: 1.5 行

ページ 19: [78] 書式を変更 作成者

フォント: 7 pt, フォントの色: テキスト 1

ページ 19: [79] 書式を変更 作成者

フォント: 7 pt, フォントの色: テキスト 1

ページ 19: [80] 書式変更 作成者

行間: 1.5 行

ページ 19: [81] 書式を変更 作成者

フォントの色: テキスト 1

ページ 19: [82] 書式変更 作成者

両端揃え, 行間: 1.5 行

ページ 19: [83] 書式を変更 作成者

フォント: 7 pt, フォントの色: テキスト 1

ページ 19: [84] 書式変更 作成者

行間: 1.5 行

ページ 19: [85] 書式を変更 作成者

フォントの色: テキスト 1

ページ 19: [86] 書式変更 作成者

両端揃え, 行間: 1.5 行

ページ 19: [87] 書式を変更 作成者

フォント: 7 pt, フォントの色: テキスト 1

ページ 19: [88] 書式変更 作成者

行間: 1.5 行

ページ 19: [89] 書式を変更 作成者



フォント : 7 pt, フォントの色 : テキスト 1

ページ 19: [89] 書式を変更 作成者

フォント : 7 pt, フォントの色 : テキスト 1

ページ 19: [90] 書式を変更 作成者

フォント : 7 pt, フォントの色 : テキスト 1

ページ 19: [91] 書式を変更 作成者

フォント : 7 pt, フォントの色 : テキスト 1

ページ 19: [92] 書式を変更 作成者

フォントの色 : テキスト 1

ページ 19: [93] 書式変更 作成者

両端揃え, 行間 : 1.5 行

ページ 19: [94] 書式を変更 作成者

フォント : 7 pt, フォントの色 : テキスト 1

ページ 19: [95] 書式変更 作成者

行間 : 1.5 行

ページ 19: [96] 書式を変更 作成者

フォントの色: テキスト 1

ページ 19: [97] 書式変更 作成者

両端揃え, 行間: 1.5 行

ページ 19: [98] 書式を変更 作成者

フォント: 7 pt, フォントの色: テキスト 1

ページ 19: [99] 書式変更 作成者

行間: 1.5 行

ページ 19: [100] 書式を変更 作成者

フォントの色: テキスト 1

ページ 19: [101] 書式変更 作成者

両端揃え, 行間: 1.5 行

ページ 19: [102] 書式を変更 作成者

フォント: 7 pt, フォントの色: テキスト 1

ページ 19: [103] 書式変更 作成者

行間: 1.5 行

ページ 19: [104] 書式を変更 作成者

フォントの色: テキスト 1

ページ 19: [105] 書式変更 作成者

両端揃え, 行間: 1.5 行

ページ 19: [106] 書式を変更 作成者

フォント: 7 pt, フォントの色: テキスト 1

ページ 19: [107] 書式変更 作成者

行間: 1.5 行

ページ 19: [108] 書式を変更 作成者

フォントの色: テキスト 1

ページ 19: [109] 書式変更 作成者

両端揃え, 行間: 1.5 行

ページ 19: [110] 書式を変更 作成者

フォント: 7 pt, フォントの色: テキスト 1

ページ 19: [111] 書式変更 作成者

行間：1.5 行

ページ 19: [112] 書式を変更 作成者

フォントの色：テキスト 1

ページ 19: [113] 書式変更 作成者

両端揃え, 行間：1.5 行

ページ 19: [114] 書式を変更 作成者

フォント：7 pt, フォントの色：テキスト 1

ページ 19: [115] 書式変更 作成者

行間：1.5 行

ページ 19: [116] 書式を変更 作成者

フォントの色：テキスト 1

ページ 19: [117] 書式変更 作成者

両端揃え, 行間：1.5 行

ページ 19: [118] 書式を変更 作成者

フォント：7 pt, フォントの色：テキスト 1

ページ 19: [119] 書式変更 作成者

行間: 1.5 行

ページ 19: [120] 書式を変更 作成者

フォントの色: テキスト 1

ページ 19: [121] 書式変更 作成者

両端揃え, 行間: 1.5 行

ページ 19: [122] 書式を変更 作成者

フォント: 7 pt, フォントの色: テキスト 1

ページ 19: [123] 書式変更 作成者

行間: 1.5 行

ページ 19: [124] 書式を変更 作成者

フォントの色: テキスト 1

ページ 19: [125] 書式変更 作成者

両端揃え, 行間: 1.5 行

ページ 19: [126] 書式を変更 作成者

フォント: 7 pt, フォントの色: テキスト 1

ページ 19: [127] 書式変更 作成者

行間: 1.5 行

ページ 19: [128] 書式を変更 作成者

フォントの色: テキスト 1

ページ 19: [129] 書式変更 作成者

両端揃え, 行間: 1.5 行

ページ 19: [130] 書式を変更 作成者

フォント: 7 pt, フォントの色: テキスト 1

ページ 19: [131] 書式変更 作成者

行間: 1.5 行

ページ 19: [132] 書式を変更 作成者

フォントの色: テキスト 1

ページ 19: [133] 書式変更 作成者

両端揃え, 行間: 1.5 行

ページ 19: [134] 書式を変更 作成者

フォント: 7 pt, フォントの色: テキスト 1

ページ 19: [135] 書式変更 作成者

行間: 1.5 行

ページ 19: [136] 書式を変更 作成者

フォントの色: テキスト 1

ページ 19: [137] 書式変更 作成者

両端揃え, 行間: 1.5 行

ページ 19: [138] 書式を変更 作成者

フォント: 7 pt, フォントの色: テキスト 1

ページ 19: [139] 書式変更 作成者

行間: 1.5 行

ページ 19: [140] 書式を変更 作成者

フォントの色: テキスト 1

ページ 19: [141] 書式変更 作成者

両端揃え, 行間: 1.5 行

ページ 19: [142] 書式を変更 作成者

フォント: 7 pt, フォントの色: テキスト 1

ページ 19: [143] 書式変更 作成者

行間: 1.5 行

ページ 19: [144] 書式を変更 作成者

フォントの色: テキスト 1

ページ 19: [145] 書式変更 作成者

両端揃え, 行間: 1.5 行

ページ 19: [146] 書式を変更 作成者

フォント: 7 pt, フォントの色: テキスト 1

ページ 19: [147] 書式変更 作成者

行間: 1.5 行

ページ 19: [148] 書式を変更 作成者

フォント: 7 pt, フォントの色: テキスト 1

ページ 19: [149] 書式を変更 作成者

フォント: 7 pt, フォントの色: テキスト 1



ページ 19: [150] 書式を変更 作成者

フォント: 7 pt, フォントの色: テキスト 1

ページ 19: [151] 書式変更 作成者

行間: 1.5 行

ページ 19: [152] 書式を変更 作成者

フォントの色: テキスト 1

ページ 19: [153] 書式変更 作成者

両端揃え, 行間: 1.5 行

ページ 19: [154] 書式を変更 作成者

フォント: 7 pt, フォントの色: テキスト 1

ページ 19: [155] 書式変更 作成者

行間: 1.5 行

ページ 19: [156] 書式を変更 作成者

フォントの色: テキスト 1

ページ 19: [157] 書式変更 作成者

両端揃え, 行間: 1.5 行

ページ 19: [158] 書式を変更 作成者

フォント: 7 pt, フォントの色: テキスト 1

ページ 19: [159] 書式変更 作成者

行間: 1.5 行

ページ 19: [160] 書式を変更 作成者

フォントの色: テキスト 1

ページ 19: [161] 書式変更 作成者

両端揃え, 行間: 1.5 行

ページ 19: [162] 書式を変更 作成者

フォント: 7 pt, フォントの色: テキスト 1

ページ 19: [163] 書式変更 作成者

行間: 1.5 行

ページ 19: [164] 書式を変更 作成者

フォントの色: テキスト 1

ページ 19: [165] 書式変更 作成者

両端揃え, 行間: 1.5 行

ページ 19: [166] 書式を変更 作成者

フォント: 7 pt, フォントの色: テキスト 1

ページ 19: [167] 書式変更 作成者

行間: 1.5 行

ページ 19: [168] 書式を変更 作成者

フォント: 7 pt, フォントの色: テキスト 1

ページ 19: [169] 書式変更 作成者

行間: 1.5 行

ページ 19: [170] 書式を変更 作成者

フォントの色: テキスト 1

ページ 19: [171] 書式変更 作成者

両端揃え, 行間: 1.5 行

ページ 19: [172] 書式を変更 作成者

フォント: 7 pt, フォントの色: テキスト 1

ページ 19: [173] 書式変更 作成者

行間: 1.5 行

ページ 19: [174] 書式を変更 作成者

フォントの色: テキスト 1

ページ 19: [175] 書式変更 作成者

両端揃え, 行間: 1.5 行

ページ 19: [176] 書式を変更 作成者

フォント: 7 pt, フォントの色: テキスト 1

ページ 19: [177] 書式変更 作成者

行間: 1.5 行

ページ 19: [178] 書式を変更 作成者

フォントの色: テキスト 1

ページ 19: [179] 書式変更 作成者

両端揃え, 行間: 1.5 行

ページ 19: [180] 書式を変更 作成者

フォント: 7 pt, フォントの色: テキスト 1

ページ 19: [181] 書式変更 作成者

行間: 1.5 行

ページ 19: [182] 書式を変更 作成者

フォントの色: テキスト 1

ページ 19: [183] 書式変更 作成者

両端揃え, 行間: 1.5 行

ページ 19: [184] 書式を変更 作成者

フォント: 7 pt, フォントの色: テキスト 1

ページ 19: [185] 書式変更 作成者

行間: 1.5 行

ページ 19: [186] 書式を変更 作成者

フォントの色: テキスト 1

ページ 19: [187] 書式変更 作成者

両端揃え, 行間: 1.5 行

ページ 19: [188] 書式を変更 作成者

フォント: 7 pt, フォントの色: テキスト 1

ページ 19: [189] 書式変更 作成者

行間: 1.5 行

ページ 19: [190] 書式を変更 作成者

フォントの色: テキスト 1

ページ 19: [191] 書式変更 作成者

両端揃え, 行間: 1.5 行

ページ 19: [192] 書式を変更 作成者

フォント: 7 pt, フォントの色: テキスト 1

ページ 19: [193] 書式変更 作成者

行間: 1.5 行

ページ 19: [194] 書式を変更 作成者

フォント: Arial, 7 pt, フォントの色: テキスト 1, 英語 (米国)

ページ 19: [194] 書式を変更 作成者

フォント: Arial, 7 pt, フォントの色: テキスト 1, 英語 (米国)

ページ 19: [195] 書式を変更 作成者

フォント : Arial, 7 pt, フォントの色 : テキスト 1, 英語 (米国)

ページ 19: [195] 書式を変更 作成者

フォント : Arial, 7 pt, フォントの色 : テキスト 1, 英語 (米国)

ページ 19: [196] 書式を変更 作成者

フォント : Arial, 7 pt, フォントの色 : テキスト 1, 英語 (米国)

ページ 19: [196] 書式を変更 作成者

フォント : Arial, 7 pt, フォントの色 : テキスト 1, 英語 (米国)

ページ 19: [197] 書式を変更 作成者

フォント : Arial, 7 pt, フォントの色 : テキスト 1, 英語 (米国)

ページ 19: [197] 書式を変更 作成者

フォント : Arial, 7 pt, フォントの色 : テキスト 1, 英語 (米国)

ページ 19: [198] 書式を変更 作成者

フォント : Arial, 7 pt, フォントの色 : テキスト 1, 英語 (米国)

ページ 19: [198] 書式を変更 作成者

フォント : Arial, 7 pt, フォントの色 : テキスト 1, 英語 (米国)

ページ 19: [199] 書式を変更 作成者

フォント : Arial, 7 pt, フォントの色 : テキスト 1, 英語 (米国)

ページ 19: [199] 書式を変更 作成者

フォント : Arial, 7 pt, フォントの色 : テキスト 1, 英語 (米国)

ページ 19: [200] 書式を変更 作成者

フォント : Arial, 7 pt, フォントの色 : テキスト 1, 英語 (米国)

ページ 19: [200] 書式を変更 作成者

フォント : Arial, 7 pt, フォントの色 : テキスト 1, 英語 (米国)

ページ 19: [201] 書式を変更 作成者

フォント : Arial, 7 pt, フォントの色 : テキスト 1, 英語 (米国)

ページ 19: [201] 書式を変更 作成者

フォント : Arial, 7 pt, フォントの色 : テキスト 1, 英語 (米国)

ページ 19: [202] 書式を変更 作成者

フォント : Arial, 7 pt, フォントの色 : テキスト 1, 英語 (米国)



ページ 19: [202] 書式を変更 作成者

フォント : Arial, 7 pt, フォントの色 : テキスト 1, 英語 (米国)

ページ 19: [203] 書式を変更 作成者

フォント : 7 pt, フォントの色 : テキスト 1

ページ 19: [204] 書式を変更 作成者

フォント : Arial, 7 pt, フォントの色 : テキスト 1, 英語 (米国)

ページ 19: [204] 書式を変更 作成者

フォント : Arial, 7 pt, フォントの色 : テキスト 1, 英語 (米国)

ページ 19: [205] 書式を変更 作成者

フォント : 7 pt, フォントの色 : テキスト 1

ページ 19: [205] 書式を変更 作成者

フォント : 7 pt, フォントの色 : テキスト 1